Dynamics of four-wheel-drive electric vehicle during machine fault condition

P. Nussbaumer[1], C. Macek[1], M. Ploechl[2] and T.M. Wolbank[1]
Vienna University of Technology
[1]Institute of Energy Systems and Electrical Drives
[2]Institute of Mechanics and Mechatronics
Gusshausstr. 25-29 / 370-2
1040 Vienna, Austria
Tel.: +43 (1) – 58801 370226
Fax: +43 (1) – 58801 9370226
E-mail: thomas.wolbank@tuwien.ac.at

Acknowledgements

The work to this investigation was supported by Vienna University of Technology as part of the doctoral college Energy Systems 2030.

Keywords

«Electric vehicle», «Electrical drive», «Fault handling strategy», «Safety», «Simulation»

Abstract

The need of carbon dioxide reduction led to increasing interest in the electric car. The shift from conventional to electric cars by simply replacing the internal combustion engine (ICE) with an electric machine might not be the best solution. Thus, new system designs like four-in-wheel drives are evolving. Although generally highly reliable, a failure in the electric machine can lead to dangerous driving situations. Depending on the type of the occurring fault different influence on for example the machine torque can be investigated. Examples for these effects are constant braking torque, torque ripple or blocking of the rotor. This results in possible reduction of driving stability. The road condition and current driving behavior (cornering, acceleration, etc.) influences the driving stability during fault condition. The effects of fault conditions on vehicle dynamics are thus investigated in the publication at hand.

Introduction

The electric car is going to play an important role to reduce carbon dioxide emission and energy consumption in the transportation sector. In the most common configuration electric vehicles (EVs) are powered from one main drive and a gearbox is transferring the torque to the wheels. An attractive possibility is the application of a single drive per wheel either constructed as in-wheel drives or individual drives with gearbox and a short shaft connected to the wheel. Such designs offer new possibilities in driving dynamics and construction. It is frequently applied in light electric vehicles.

Although generally highly reliable a failure in one of the electrical machines may lead to dangerous situations in traffic. Furthermore the drive consists of different components like inverter and sensors (current, speed,…) that may fail and lead to problems in the control of the machine. The concept of applying individual drives offers the possibility to ensure safe operation and switch to emergency operation allowing reaching home or the next garage with the remaining healthy drives.

Faults occurring in an electric drive may lead to torque ripples, high braking torque or sudden torque collapse. Thus, electric drive faults may result in instability of the vehicle motion and dangerous situations in traffic. The analysis of effects on vehicle dynamics during a fault occurring in one of the machines in the four-wheel-drive system has not been sufficiently covered in literature so far.

In [1] and [2] different EV-concepts with more than one drive installed are compared concerning the behavior during a sudden torque collapse. The different concepts are analyzed for this fault occurring in one drive during acceleration and cornering for various road conditions. The compared EV-concepts are a two-in-wheel and a four-in-wheel motor drive-type and a FRID (front-and-rear-wheel-independent-drive-type) EV. The last concept has been proposed in [3], for instance. It is concluded that the FRID EV is the only vehicle that shows stable driving dynamics even when a fault occurs. In case of the other two EV-concepts dangerous driving conditions arise in the event of a failure in one motor.

In [4] an emergency scenario is investigated where the motor in a four-wheel drive type EV on the same axis as the failing one is switched off with different delay times. However, stable operation cannot be guaranteed.

The above referenced studies deal with one fault type only – sudden torque collapse. Such a fault occurs in case of control electronics or inverter breakdown. In addition to that electric machine failures may result in torque ripple and braking torques. The latter ones may be the result of single- or multi-phase short circuits. Furthermore, a defect in the inverter can lead to braking torques if driving a permanent magnet synchronous machine (PMSM) at high speed. A torque ripple is the result of different fault conditions. Open phase [5], turn-to turn short circuit [6] or rotor-related [7] faults are among these.

To investigate the effects of the above stated failures a four-wheel simulation model is developed in MATLAB. The simulated electric vehicle is based on one of the first electric vehicles available for mass market – the Mitsubishi i-MiEV (Mitsubishi innovative electric vehicle). However, the drive-concept is changed from one main drive system only to four individual motors for each wheel. The developed model allows changing the road conditions, the occurring failure, the driving scenario and the four-wheel-concept (in-wheel drives and individual drives with gear box and short shaft). The objective of this paper is to present the used vehicle modeling and raise awareness for the issue of driving dynamics of EVs during machine fault condition. Some first simulation results for different scenarios will be presented.

The Investigated Electric Vehicle

As mentioned in the introduction the investigated electric vehicle is based on the Mitsubishi iMiEV. The mechanical dimensions and figures are kept the same. However, the drive train is changed from one electrical machine in the back of the vehicle driving the rear axle only to four machines driving each wheel individually. Two different concepts can be used to realize this. Either four in-wheel-drives can be applied or each wheel is driven by one electrical machine connected through individual gear boxes and short shafts. The latter one is chosen in this investigation.

Table I. Technical data of the Mitsubishi iMiEV and the simulated EV

Parameter	iMiEV	Simulated EV
Length	3475 mm	3475 mm
Width	1475 mm	1475 mm
Height	1610 mm	1610 mm
Wheel track	1290 mm	1290 mm
Wheelbase	2550 mm	2550 mm
Empty mass	1110 kg	1110 kg
Gross vehicle mass	1450 kg	1450 kg
Range	150 km	150 km
Limit speed	130 kph	130 kph
Acceleration 0-100km/h	15.9 s	15.9 s
Drive motor	Permanent magnet synchronous machine (PMSM)	4x PMSM
Maximum power	49kW @ 2500-8000 rpm	4x 12kW @ 2500-8000 rpm
Maximum torque	180Nm @ 0-2500 rpm	4x 45Nm @ 0-2500 rpm
Type of drive	Rear wheel drive	4x individual drives (gear box + short shaft)

The most important technical data of the Mitsubishi iMiEV applied to the simulation model developed in MATLAB is shown in Table I.

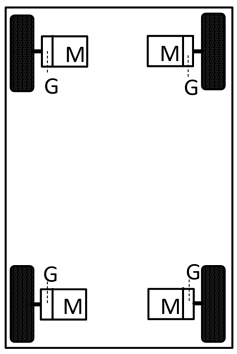

Fig. 1: Scheme of drive type of simulated EV.

The drive type used in the simulations is depicted in Fig. 1. The important difference between this concept and the in-wheel-drives is the weight distribution (higher unsprung mass of in-wheel-drive). The reduction gear ratio is chosen to seven. The tire radius is 0.3m and the limit speed is about 130kph together with the maximum rotational speed of 8000rpm for the electrical motors. The motor characteristic for the individual PMSM-drives is depicted in Fig. 2. The area of constant torque (45Nm) between 0 and 2500rpm is clearly visible. To reach higher rotational speed the PMSM has to enter the field-weakening range between 2500rpm and the maximum rotational speed of 8000rpm. This area is sometimes also denoted constant power regime.

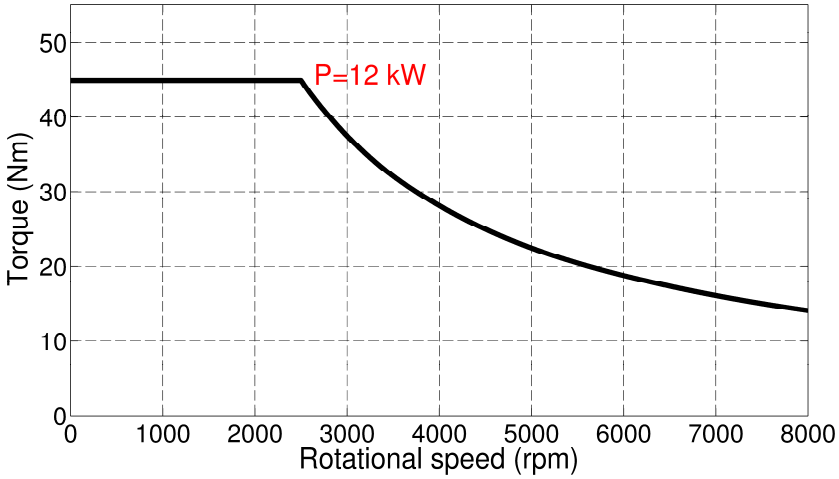

Fig. 2: Motor characteristic of individual PMSM-drives.

The Four-Wheel Simulation Model

The simulation model created in MATLAB is based on the equations presented in [8] and [9]. Due to the complexity of the simulation model used, only the most important equations are presented.

The three most important components of the simulation are the mathematical description and implementation of the horizontal and vertical dynamics and the tire model. The used concepts and some principal equations will be described in the following. As all four wheels are driven by an individual motor the two-track model is chosen. The simulation model has been tested with a step steering input, load transfer test (open loop) and the lane change maneuver.

Horizontal Dynamics

In Fig. 3 the vehicle is viewed at from the top for the mathematical description of the horizontal dynamics. The external forces and torques have to be regarded in the equations of motion. Fig. 3The indices FL, FRi, RL and RRi denote the quantities affecting the front left, front right, rear left and rear right tire, respectively. Moreover, the steering angle δ_V and the center of gravity CG are shown. The movement of the center of gravity is described by the side slip angle of

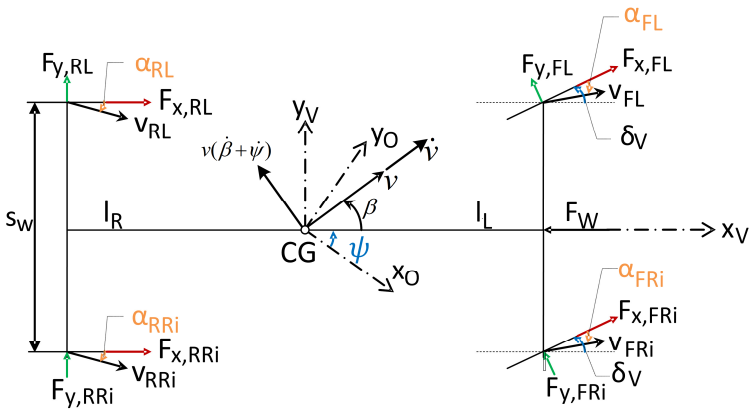

Fig. 3: Description of quantities for horizontal dynamics.

the vehicle β and the vehicle speed v. The yaw angle ψ measures the angle of rotation of the vehicle's longitudinal axis with respect to the inertial frame (x_0, y_0). In addition to that the accelerations of CG, $\dot{v}$ and $v(\dot{\beta}+\dot{\psi})$ are depicted in Fig. 3. The force F_W denotes the aerodynamic drag. Using these quantities Newton's and Euler's law can be applied. This results in the following equations.

$$\begin{aligned}&-m\cdot v(\dot{\beta}+\dot{\psi})\cdot\sin(\beta)+m\cdot\dot{v}\cdot\cos(\beta)=F_{x,RRi}+F_{x,RL}+F_{x,FL}\cdot\cos(\delta_V)+F_{x,FRi}\cdot\cos(\delta_V)-\\&-F_{y,FL}\cdot\sin(\delta_V)-F_{y,FRi}\cdot\sin(\delta_V)-F_W\end{aligned} \tag{1}$$

$$\begin{aligned}&m\cdot v(\dot{\beta}+\dot{\psi})\cdot\cos(\beta)+m\cdot\dot{v}\cdot\sin(\beta)=F_{y,RRi}+F_{y,RL}+F_{x,FL}\cdot\sin(\delta_V)+F_{x,FRi}\cdot\sin(\delta_V)+\\&+F_{y,FL}\cdot\cos(\delta_V)+F_{y,FRi}\cos(\delta_V)\end{aligned} \tag{2}$$

$$\begin{aligned}&J_z\cdot\ddot{\psi}=-F_{y,RL}\cdot l_R-F_{y,RRi}\cdot l_R+F_{y,FL}\cdot\cos(\delta_V)\cdot l_F+F_{y,FRi}\cdot\cos(\delta_V)\cdot l_F-F_{x,RL}\cdot\frac{s_w}{2}+\\&+F_{x,RRi}\cdot\frac{s_w}{2}+F_{y,FL}\cdot\sin(\delta_V)\cdot\frac{s_w}{2}-F_{y,FRi}\cdot\sin(\delta_V)\cdot\frac{s_w}{2}-F_{x,FL}\cdot\cos(\delta_V)\cdot\frac{s_w}{2}+\\&+F_{x,FRi}\cdot\sin(\delta_V)\cdot\frac{s_w}{2}+F_{x,FL}\cdot\sin(\delta_V)\cdot l_F+F_{x,FRi}\cdot\sin(\delta_V)\cdot l_F\end{aligned} \tag{3}$$

The quantities m, s_W, and J_Z describe the vehicle mass, wheel track and moment of inertia, respectively.

Vertical Dynamics

The important quantities are the wheel loads F_Z. The equations for calculation of the wheel loads read:

$$F_{z,FL}=m\cdot\frac{g}{2}\cdot\frac{l_R}{l}-c_{roll}\cdot c_{total,\kappa}\cdot\frac{s_w}{2}\cdot\frac{\kappa}{2}+c_{total,\varphi}\cdot\frac{l}{2}\cdot\frac{\varphi}{4}-F_W\cdot\frac{h_W}{l} \tag{4}$$

$$F_{z,FRi}=m\cdot\frac{g}{2}\cdot\frac{l_R}{l}+c_{roll}\cdot c_{total,\kappa}\cdot\frac{s_w}{2}\cdot\frac{\kappa}{2}+c_{total,\varphi}\cdot\frac{l}{2}\cdot\frac{\varphi}{4}-F_W\cdot\frac{h_W}{l} \tag{5}$$

$$F_{z,RL}=m\cdot\frac{g}{2}\cdot\frac{l_F}{l}-(1-c_{roll})\cdot c_{total,\kappa}\cdot\frac{s_w}{2}\cdot\frac{\kappa}{2}-c_{total,\varphi}\cdot\frac{l}{2}\cdot\frac{\varphi}{4}-F_W\cdot\frac{h_W}{l} \tag{6}$$

$$F_{z,RRi}=m\cdot\frac{g}{2}\cdot\frac{l_F}{l}+(1-c_{roll})\cdot c_{total,\kappa}\cdot\frac{s_w}{2}\cdot\frac{\kappa}{2}-c_{total,\varphi}\cdot\frac{l}{2}\cdot\frac{\varphi}{4}-F_W\cdot\frac{h_W}{l} \tag{7}$$

The constants c_{roll}, $c_{total,\kappa}$ and $c_{total,\varphi}$ define the ratio between the stabilizers in the front and in the rear and the total spring constant for roll and pitch, respectively. In the model they are chosen to 0.62, 95000N/m and 87500N/m. The equations consists of a portion determined by the vehicle mass m, Newton's constant g and the length between CG and the rear l_R or front l_F axis and the wheel base l. Furthermore the derivation of the vertical loads is based on steady state cornering with pitch angle φ and roll angle κ angle.

A more detailed description can also be found in [8] and [10].

Tires

The tire model describes the force transfer between vehicle and road. Thus, the modeling of the tires is a very crucial part in vehicle dynamic simulations. For these investigations the HSRI (Highway Safety Research Institute) model is chosen as this is a good compromise between computational burden and accuracy. It is described in [8] more detailed. However, the HSRI-model only describes the steady state of the tire forces. The transient behavior is included by the following equation

$$\frac{\sigma_y}{v_x}\cdot\dot{\alpha}_i'+\alpha_i'=\alpha_i \tag{8}$$

The variable σ_y describes the relaxation length and is chosen constant to 0.25m. The longitudinal speed of the tire's center is v_x. α_i' and α_i are the transient and steady state (output of HSRI-model) side slip angle of the respective tire. The consideration of the transient behavior is needed for simulation of the failures resulting in torque ripple, for example. For more detailed explanations see [10].

Vehicle Dynamics for Simulated Fault Conditions

The concept of four individual drives in one electric vehicle obviously has many advantages concerning new degrees of freedom for the control and thus, better dynamic performance and room layout. However, other than for conventional vehicles with one drive only, the force is not distributed equally on both wheels of one axis due to the lack of a differential gear. Thus, in case of machine failure the resulting changes in torque distribution among the four drives can lead to dangerous driving situations if no precautions have been implemented. The effects of drive breakdown are investigated for the vehicle model described in the previous sections. Two different fault scenarios are analyzed – negative (braking) torque and torque ripple in one drive system during cornering. The first few seconds after occurrence of a fault are analyzed. For the driver it is hard to immediately react on changes within the first second [11].

Negative Torque During Cornering

In this section the effect of a negative torque on the vehicle dynamics suddenly occurring in one electrical drive is analyzed. Reasons for such faults can be one or multi phase short circuits, breakdown of the inverter at high speed (e.g. PMSM in field weakening area), etc.. In this scenario the vehicle is cornering with a steering wheel angle of 74° (steering angle of 3.9°). The vehicle speed is 13.9m/s (50kph). The failure occurs after one second (at t=0s). The simulation is already in a steady state. The total simulation time is four seconds. The location of failure is varied between the rear left and right wheel. The road surface condition is dry.

The suddenly occurring negative torque is set to ~-36Nm (mechanical torque of electrical machine, equaling a braking torque of ~255Nm at the wheel). The fault occurring on the rear left drive influences the vehicle driving dynamics the most. The EV leaves the current driving lane by 0.19m to the left and starts skidding if the driver does not react in the first second after failure occurrence. In case of failure in the rear right wheel drive the EV leaves the lane to the right by 0.18m after one second. The trajectory of the vehicle's center of gravity for faultless and faulty driving condition during cornering is depicted in Fig. 4.

The green trace shows the trajectory of the faultless condition during cornering. The solid red and solid dashed lines show the trajectory for a failure (negative torque) occurring in the rear right and rear left wheel drive, respectively. The vehicle's position and orientation is depicted for all investigated scenarios at the occurrence of the fault (t=0s), after one second (t=1s) and after two seconds (t=2s) as red and green rectangles. The vehicle is already displaced from its faultless position if the driver does not react within one second. A reaction within two seconds by the driver or a fault handling system is essential to maintain safe driving condition for both fault scenarios as the vehicle would leave its lane.

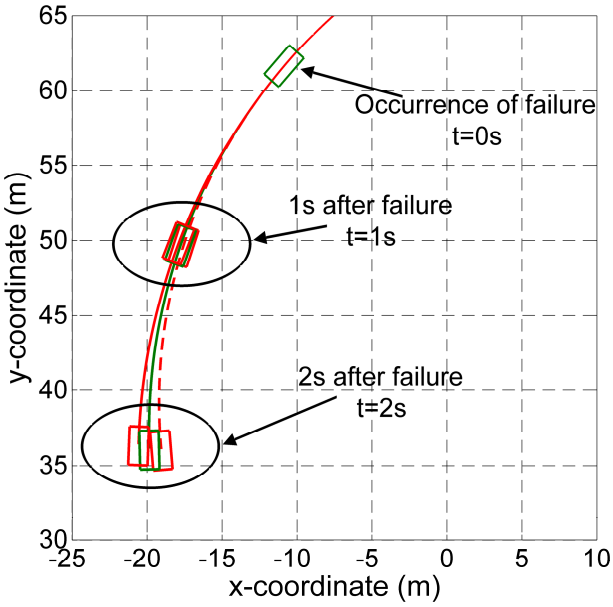

Fig. 4: Trajectory of center of gravity for faultless condition (green) and failure occurring in rear right (solid, red) and left (dashed, red) wheel drive at t=0s during cornering; Fault condition: negative torque.

An important parameter that has to be investigated to assess the vehicle's stability is the yaw rate. It is depicted in Fig. 5 during faultless and different fault conditions.

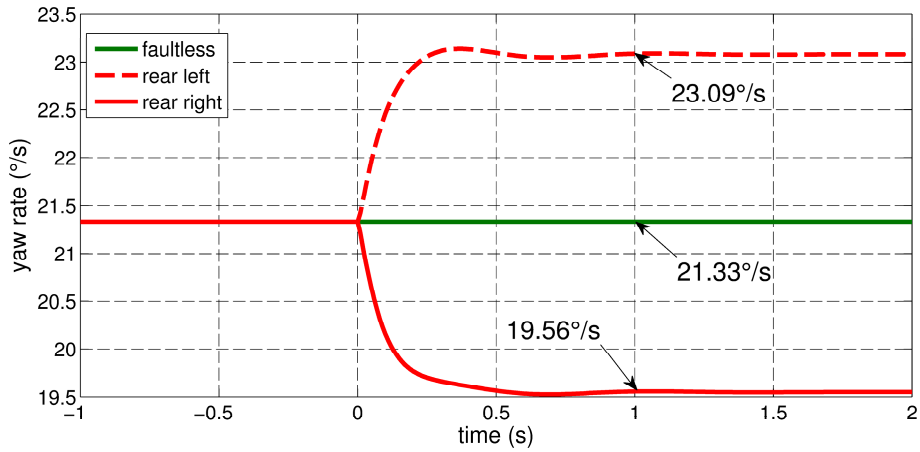

Fig. 5: Yaw rate for faultless (green) and failure occurring in rear left (red, dashed) and right (red, solid) wheel drive at t=0s; Fault condition: negative torque.

The values of the yaw rates at t=1s are marked in the figure. In this interval of one second after fault occurrence it is difficult for the driver to react. The difference of yaw rate between the faultless (yaw rate: 21.33°/s) and the negative torque occurring at the rear left (yaw rate: 23.09°/s) and right (yaw rate: 19.56°/s) wheel drive one second after the fault occurrence is determined to 1.76°/s and 1.77°/s, respectively.

In Fig. 6(a) and (b) the side slip angle for faultless condition (green traces) and the two investigated fault scenarios (red traces) with negative torque occurring in the rear left and rear right wheel drive are shown, respectively.

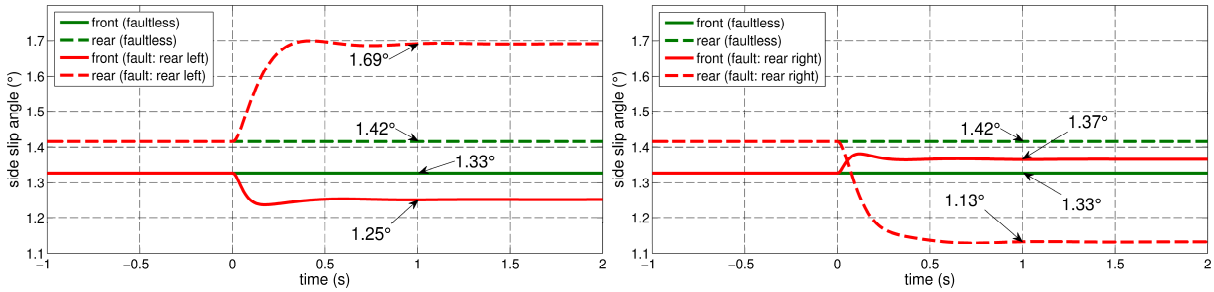

(a) (b)

Fig. 6: Side slip angle of front (solid) and rear (dashed) wheels for faultless (green) and failure occurring in rear (a) left and (b) right wheel drive at t=0s (red); Fault condition: negative torque.

For the scenario with negative torque occurring in the rear right wheel drive the side slip angles for the front and rear tires after one second can be identified to 1.37° and 1.13°, respectively. Thus, the change for this fault scenario in comparison to the faultless situation is 0.04° and 0.29°, respectively The side slip angle one second after negative torque occurring in the rear left wheel drive changes by 0.08° and 0.27° (from 1.33° and 1.25° to 1.42° and 1.69°) for the front and rear wheels, respectively.

The side slip angle of the vehicle changes by 0.11° (from 0.42° to 0.31°) for failure scenario occurring in the rear left and by 0.13° (from 0.42° to 0.55°) for occurring failure in the rear right wheel drive after one second. The side slip angle of the vehicle over time for the investigated scenarios is depicted in Fig. 7(a).
The lateral acceleration has increased from 5.17m/s^2 to 5.57m/s^2 (by 0.40m/s^2) in case of the scenario with the rear left failing one second after occurrence. In case of a drive failure occurring in the rear right wheel drive the lateral acceleration changes by 0.45m/s^2 from 5.17m/s^2 to 4.72m/s^2. The corresponding traces are depicted in Fig. 7(b).

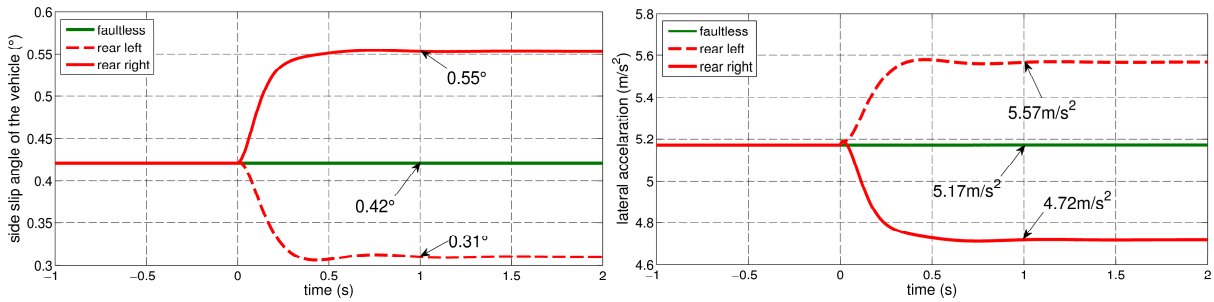

(a) (b)

Fig. 7: (a) Side slip angle of the vehicle and (b) lateral acceleration for faultless (green) and failure occurring in rear right (red, solid) and left (red, dashed) wheel drive at t=0s (red); Fault condition: negative torque.

Regarding the results shown for negative torque occurring in one of the rear drives of an electrical vehicle with four individual drives it can be concluded that in cornering case a breaking torque due to electrical drive failure leads to similar results for both investigated scenario (failure in rear left or right wheel drive) in terms of danger for driving stability.

Torque Ripple During Cornering

The second investigated scenario is a suddenly occurring torque ripple. This failure may occur due to an open-phase fault [5], a turn-to-turn short circuit (with higher ripple magnitude) [6] or rotor-related faults [7].

The torque ripple applied in this scenario has a time period of 0.05s. The minimum of the applied torque ripple in one of the four electrical machines is chosen to -10% of the machine's maximum torque in this operating point (~-2Nm mechanical torque of electrical machine). The maximum is the

actual demanded torque. The results for such a fault occurring in the rear left or right wheel drive are analyzed in this section.

Hardly any deviation from the faultless track can be detected in both investigated cases. The trajectories of the center of gravity during the different investigated scenarios are depicted in Fig. 8. The rectangles again show the position of the vehicle at the time of failure occurrence (t=0s), one second after failure occurrence (t=1s) and two seconds after failure occurrence (t=2s). In comparison to the scenario with negative torque occurring during cornering as analyzed in the previous section the displacement of the vehicle due to machine failure in one drive is much lower and hardly detectable.

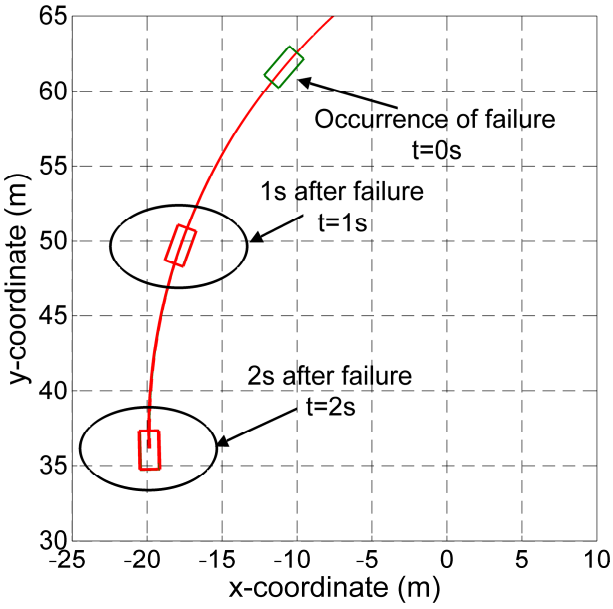

Fig. 8: Trajectory of center of gravity for faultless condition (green) and failure occurring in rear right (solid, red) and left (dashed, red) wheel drive at t=0s during cornering; fault condition: torque ripple.

Again the yaw rate for the different investigated scenarios has been analyzed.
Fig. 9 shows the resulting yaw rate for failure scenario occurring in the rear left (red, dashed) and rear right (red, solid) wheel drive in comparison to the faultless situation (green).

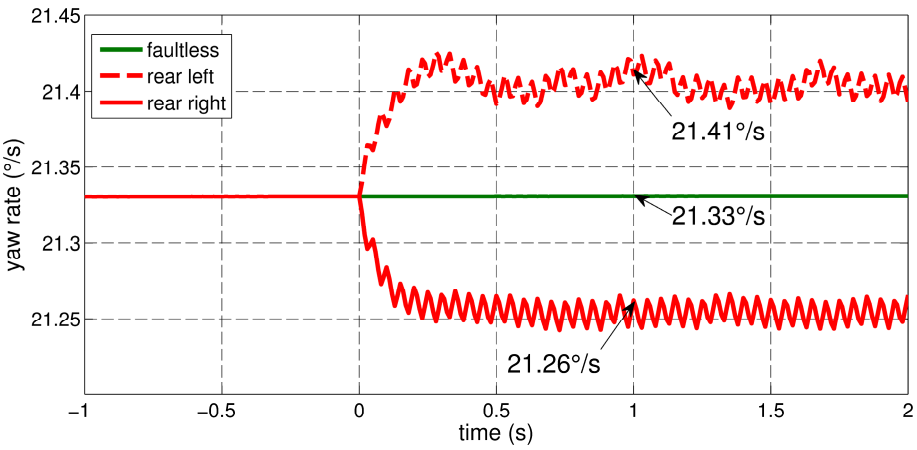

Fig. 9: Yaw rate for faultless (green) and failure occurring in rear left (red, dashed) and right (red, solid) wheel drive at t=0s; fault condition: torque ripple.

The yaw rate changes from the faultless situation (green; 21.33°/s) to the scenario with torque ripple occurring at the rear left (red, dashed; 21.41°/s) and right (red, solid; 21.26°/s) wheel drive by 0.08°/s

and 0.07°/s after one second, respectively. This is much lower than for the negative torque failure described in the previous section.

Analyzing the side slip angle for the investigated scenarios results in the traces illustrated in Fig. 10. The resulting side slip angles of the front (solid) and rear (dashed) axle are shown for the faultless situation (green) and occurring torque ripple (red) in the rear left (Fig. 10(a)) and rear right (Fig. 10(b)) wheel drive.

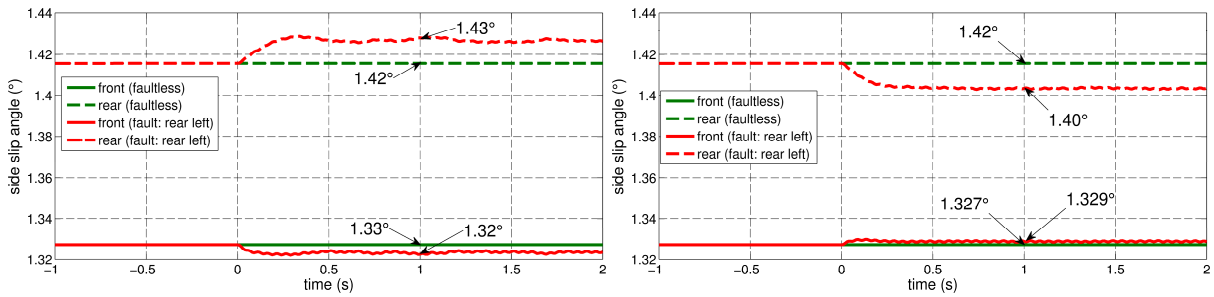

(a) (b)

Fig. 10: Side slip angle of front (solid) and rear (dashed) wheels for faultless (green) and failure occurring in rear (a) left and (b) right wheel drive at t=0s (red); fault condition: torque ripple.

The change of side slip angle between the faultless situation and the failure occurring at the rear left drive can be determined to 0.01° for the rear (from 1.42° to 1.43°) and front (from 1.33° to 1.32°) wheels, respectively. A torque ripple occurring in the rear right wheel drive leads to a change of the side slip angle after one second by 0.02° for the rear (from 1.42° to 1.40°) and 0.002° for the rear axle (from 1.327° to 1.329°). The change of the side slip angle is negligibly low in comparison to the scenarios with occurring negative torque.

The side slip angle of the vehicle obtained in the simulations carried out for the different scenarios is depicted in Fig. 11(a). The green trace shows the trace for the faultless situation, red dashed and solid the ones for the fault occurring in the rear left and rear right wheel drive, respectively.

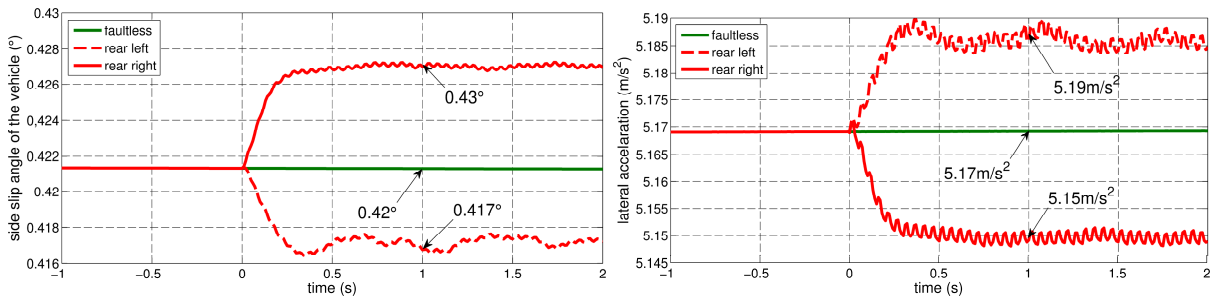

(a) (b)

Fig. 11: (a) Side slip angle of the vehicle and (b) lateral acceleration for faultless (green) and failure occurring in rear right (red, solid) and left (red, dashed) wheel drive at t=0s (red); Fault condition: torque ripple.

In case of the fault occurring in the rear left wheel the side slip angle of the vehicle changes by 0.004° (from 0.421° to 0.417°) after one second. In case of the failure occurring in the rear right wheel it changes by 0.006° only (from 0.421° to 0.427°).

In Fig. 11(b) the lateral acceleration is depicted for the different investigated scenarios. The lateral acceleration is only changed slightly for both investigated fault scenarios. The scenario with occurring fault in the rear left and right drive show a change from 5.17m/s^2 to 5.19m/s^2 and 5.15m/s^2 after one second, respectively.

Summarizing the obtained results for occurring torque ripple in the rear wheel drives during cornering generally show only slight changes of the driving dynamics. In any case the suddenly occurring negative (braking) torque is a more severe situation than torque ripple.

Conclusion

The paper presents simulation results for a four-wheel-drive electric vehicle under fault condition of a single electrical drive. Two different scenarios are investigated – a suddenly occurring negative torque and a torque ripple. Only the scenario with negative torque applied leads to a significant deviation of the vehicle's track from the faultless situation.

The paper shows that without precautions, faults occurring in one of the electrical traction drives in four-wheel electric vehicles can lead to dangerous situations. This has to be considered in the design stage of such EVs. Thus, concepts like continuous condition monitoring and incipient fault detection, as well as torque vectoring or similar methods that adequately distribute the torque on the different wheels have to be implemented.

References

[1] Mutoh, N.; Nakano, Y.; "Dynamics of Front-and-Rear-Wheel-Independent-Drive-Type Electric Vehicles at the Time of Failure," *IEEE Transactions on Industrial Electronics,* vol.59, no.3, pp.1488-1499, 2012.

[2] Mutoh, N.; Nakano, Y.; "Dynamic characteristic analyses of the front-and rear-wheel independent-drive-type electric vehicle (FRID EV) when the drive system failed during running under various road conditions," *IEEE Vehicle Power and Propulsion Conference, VPPC,* pp.1162-1169, 2009.

[3] Mutoh, N.; Kazama, T.; Takita, K.; "Driving characteristics of an electric vehicle system with independently driven front and rear wheels," *IEEE Transactions on Industrial Electronics,* vol.53, no.3, pp. 803- 813, 2006.

[4] Mutoh, N.; Takahashi, Y.; Tomita, Y.; "Failsafe Drive Performance of FRID Electric Vehicles With the Structure Driven by the Front and Rear Wheels Independently," *IEEE Transactions on Industrial Electronics,* vol.55, no.6, pp.2306-2315, 2008.

[5] Kianinezhad, R.; Nahid-Mobarakeh, B.; Baghli, L.; Betin, F.; Capolino, G.A.; "Torque Ripples Suppression for Six-Phase Induction Motors Under Open Phase Faults," *IEEE Industrial Electronics, IECON 2006 - 32nd Annual Conference on* , vol., no., pp.1363-1368, 2006.

[6] Soliman, H.M.; Hakim, S.M.E;. "Identification of Stator Winding Faults and Remedial Operation of Permanent Magnet Synchronous Motors with Suppress Noise and Ripple," *International Journal of Soft Computing and Engineering,* vol.2, no.4, pp.2231-2307, 2012.

[7] Nandi, S.; Bharadwaj, R.; Toliyat, H.A.; Parlos, A.G.; "Study of three phase induction motors with incipient rotor cage faults under different supply conditions," *Industry Applications Conference, Thirty-Fourth IAS Annual Meeting,* vol.3, pp.1922-1928, 1999.

[8] Mitschke, M.; Wallentowitz, H; "Dynamik der Kraftfahrzeuge," *Springer Verlag,* Berlin, 4th edition, 2004.

[9] Richter, B; "Schwerpunkte der Fahrzeugdynamik," *TÜV Rheinland GmbH,* Cologne, 1990.

[10] Pacejka, H.B.; "Tyre and vehicle dynamics," *Butterworth Heinemann,* Burlington, 2nd edition, 2007.

[11] Zang, Y.; Antonsson, E.K.; Grote, K.; "A new threat assessment measure for collision avoidance systems," *Intelligent Transportation Systems Conference, ITSC,* pp.968-975, 2006.